Formation of Insoluble Byproducts of Diclofenac using *Trametes versicolor* Laccase – Experimental Evidences and Model

R. Pype[a,*], B. Oulad Haj Amar[a], F. Debaste[a]

[a] *Department of Transfers, Interfaces and Processes, Université libre de Bruxelles, Av. F.D. Roosevelt 50, ULB CP165/67, 1050 Brussels, Belgium*

Abstract

Laccases are known to be able to oxidize recalcitrant micropoluttants present in the aquatic environment. In some cases, the formation of oligomers was observed following these oxidation reactions. In this work, the degradation of diclofenac (DCF), a non-steroidal anti-inflammatory drug, by *Trametes versicolor* laccase was investigated. The degradation of DCF was found to lead to the formation of brown-colored insoluble byproducts (IBs) that are suspected to be oligomers. A model based on radical polymerization was developed to describe DCF degradation and IBs formation.

Keywords: Bioremediation, Diclofenac, Laccase, Model, Polymerization, Trametes versicolor

Abbreviations

*Corresponding author
Email addresses: rosapype@ulb.ac.be (R. Pype), fdebaste@ulb.ac.be (F. Debaste)

ABTS	2,2'-azino-bis(3-ethylbenzothiazoline-6-sulfonic acid)
ACN	acetonitrile
DCF	diclofenac
DSC	differential scanning calorimetry
HPLC	high performance liquid chromatography
IBs	insoluble byproducts
LOEC	lowest observed effect concentration
metOH	methanol
NSAID	non-steroidal anti-inflammatory drug
WWTPs	wastewater treatment plants

METTRE AUSSI LES SYMBOLES DES EQUATIONS?

1. Introduction

Diclofenac (DCF) is a non-steroidal anti-inflammatory drug (NSAID) used for human health purposes [1]. This NSAID, administered topically or orally, is one of the most used worldwide [2]. Its average global consumption exceeds 1400 tons per year [1]. In some countries, DCF is also used as an all-purpose veterinary medicine for domestic livestock [1].

While most of DCF is directly washed of after dermal application, less than 1% of an orally administered dose is excreted as un-metabolized DCF [3]. Either way, an important amount of DCF ends up in wastewater treatment plants (WWTPs). However, the removal efficiency of DCF in current WWTPs ranges from 0% up to 80% and is mainly in the range between 21% and 40% [4]. So, the high consumption, incomplete assimilation and generally poor elimination in WWTPs of DCF leads to its continuous release in the aquatic environment. Nowadays, DCF contamination of surface waters, groundwaters and drinking waters spreads worldwide in concentrations ranging from ng/L to µg/L [3, 4].

As a consequence of the pseudo-persistence of DCF in the environment the aquatic organisms are chronically exposed. Some of the reported values of lowest observed effect concentration (LOEC) (0.01 µg/L to 5 µg/L) approach levels observed in wastewater effluents (0.005 µg/L to 5.5 µg/L) [1, 3]. For example, the LOEC for cytological alterations in rainbow trout (*Oncorhynchus mykiss*) liver, kidney and gills was determined to be 1 µg/L [5]. Moreover, DCF has been shown to bioaccumulate in fish [6, 7] and invertebrates [8] at environmentally relevant concentrations, which could lead to toxicity in higher trophic level organisms. Another toxicity issue arises from the presence of pharmaceuticals in the environment as multi-component mixtures. That situation can lead to bigger ecotoxicity issues [9, 10]. For instance, it was reported that a mixture of DCF with ibuprofen, naproxen, and acetylsalicylic acid had a considerable toxicity to the planktonic crustacean *Daphnia* and to the planktonic green alga *Scenedesmus subspicatus*, even at concentrations at which the single substances showed no or only very slight effects [11].

An efficient way to treat DCF in water could be the use of laccases. Laccases are lignin-modifying enzymes from the multi-copper oxidases family [12, 13]. Laccases are able to oxidize, polymerize or transform phenolic and anthropogenic compounds to less toxic derivatives [14]. Their substrates include a broad range of highly recalcitrant compounds (dyes, pesticides, endocrine disrupters, etc.) that they are able to oxidize into radicals using molecular oxygen as an electron acceptor [14, 15]. The formed reactive radicals can then undergo non-enzymatic reactions including dimerization, oligomerization and polymerization [16].

Recently, several researchers investigated the laccase-catalyzed degradation of DCF showing promising results [17–22]. In addition, some researchers reported qualitatively the formation of insoluble byproducts (IBs) [23, 24]. The formation of insoluble byproducts is an interesting point to investigate as they could be separated from the water before release in the environment. Moreover, these IBs could give us information about the degradation mechanism of DCF

Table 1: Summary of the experimental conditions and performed analyses. θ is defined by equation (13) and calculated using the values from Table 2. X_{min} is calculated following (19). t_{min} is calculated by injecting X_{min} in (17).

Name	Conditions					HPLC Analyzes	IBs Formation Analyzes
	DCF_0 (g/L)	E (U/L)	θ	X_{min}	t_{min} (h)		
EXP1	0.5	3500	0.28	0.24	2.2	3	5
EXP2	0.5	1750	0.20	0.18	2.3	3	3
EXP3	0.5	1200	0.16	0.15	2.4	0	3
EXP4	0.375	1750	0.23	0.2	3.0	0	3
EXP5	0.25	1750	0.28	0.24	4.4	0	1
EXP6	0.15	3000	0.47	0.37	6.5	3	0
EXP7	0.005	3000	2.56	0.88	70.5	2	0

by the laccase.

In this work, the formation kinetics of DCF IBs in a batch reactor and their relation with the laccase-catalyzed degradation of DCF were investigated through the evolution of the dry weigh of IBs, HPLC analyzes and differential scanning calorimetry (DSC) of IBs. On this basis, a phenomenological kinetic model was developed to describe both DCF degradation and IBs formation.

2. Materials and Methods

2.1. Materials

Most chemicals, i.e., DCF, 2,2'-azino-bis(3-ethylbenzothiazoline-6-sulfonic acid) (ABTS), $NaH_2PO_4 \cdot 2\,H_2O$, $Na_2HPO_4 \cdot 7\,H_2O$, H_3PO_4, sodium azide, NaOH, methanol (metOH) and free laccases from *Trametes versicolor* were purchased from Sigma-Aldrich (Belgium). Enzymes were presented as a powder with an activity of 12.9 U/mg or of 1.06 U/mg depending of the lot. Acetonitrile of HPLC grade (ACN) was purchased from VWR (Belgium). All reaction media were buffered at pH 7.0 (phosphate buffer prepared according to [25]) except for laccase activity assays. The Whatman filters used to recover insoluble particles were of grade 589/3.

2.2. Methods

2.2.1. Laccase Activity Assay

Laccase activity is defined as the amount of laccase able to oxidize 1 µmol of ABTS in a minute [26]. To determine the activity, the color change of ABTS oxidized by laccases in 100 mM Na-tartrate buffer (pH 4.5) was monitored using a spectrophotometer Hewlett Packard 8453 at a wavelength of 420 nm and in a 3-mL spectrophotometric cuvette at room temperature [27].

2.2.2. IBs Formation, Recovery and Weighing

The protocol described in this section is adapted from one developed to follow the formation of bisphenol A IBs [27]. In the present case, one experiment consisted in several identical batch reactors in parallel containing a given initial DCF concentration and enzyme activity (see Table 1), in a total volume of 0.2 L buffered at pH 7.0. All batch reactors were incubated at room temperature and under magnetic agitation throughout the reaction. Each experiment was conducted during 24h, one batch reactor corresponding to one measurement taken at 0h, 1h, 2h, 3h, 4h, 6h, 8h or 24h of reaction.

Two control reactors were present during each experiment, one without DCF and one without laccases, under the same conditions than the others. These controls are present to confirm that the formation of IBs occurs only if laccases catalyze the DCF reaction. Precipitates were recovered on filters (pre-dried under vacuum and weighed) by filtration through a Sartorius filtration station, dried under vacuum at room temperature for at least three days and then weighed.

The number of assays performed for each conditions set is presented on Table 1. The data presented in the results consist in average values with error bars indicating the variation between the maximal/minimal value recorded and the average value. Some of the measured weights were inferior to the weights of the controls, those were excluded from the average value as they were not significant regarding IBs formation.

No formal recovery and weighing of IBs was performed for EXP6 and EXP7 (see Table 1). However, qualitative observations indicated the formation of IBs after 5h of reaction in the case of EXP6. No IBs formation was observed in the case of EXP7.

2.2.3. HPLC Analysis

HPLC analyses were performed on samples from separate DCF degradation experiments. In that case, DCF degradations were performed in a jacketed batch reactor kept at 20 °C under magnetic agitation. The medium (30 mL) consisted of pH 7.0 phosphate buffer with the chosen DCF concentration and laccase activity. The reaction was initiated by adding the laccase to the reaction medium. Samples were withdrawn at 0h, 0h30, 1h, 2h, 3h, 4h, 5h, 6h, 7h, 8h and 24h of reaction. Samples were inactivated by addition of sodium azide before being centrifuged at 3900 rpm for 10 min. The supernatant was then diluted with milliQ water before performing the HPLC analysis.

Analyses were carried out using a Hitachi Primaide HPLC equipped with a UV detector and a XBridge^{TM} C18 column (4.6 mm x 50 mm, particle size 3.5 µm; Waters). The column was kept at 35 °C. The analysis was performed using a 5 min-isocratic elution program using a mix of milliQ-H_2O (50%), ACN (40%) and 0.5% H_3PO_4 (10%) as eluant. The injection volume was 90 µL and the flow rate was 3 mL/min. The detection was performed at 210 nm. METTRE UN PROFIL EN ANNEXE ?

For EXP6 and EXP7, DCF degradations were performed following a slightly different set up. DCF was dissolved in metOH to form a stock solution (5 g/L) that diluted in buffer to obtain the wanted DCF concentration rather than direct

dissolution of DCF in buffer. The proportion of metOH was kept at 6% v:v for the two sets of experiments. Samples were withdrawn at 0h, 0h30, 1h, 2h, 3h, 4h, 5h and 6h of reaction. The rest of the analysis was performed as usual.

The number of assays performed for each conditions set is presented on Table 1. The data presented in the results consist in average values with error bars indicating the variation between the maximal/minimal value recorded and the average value.

2.2.4. DSC Analysis

The IBs obtained after 24h of the reaction of 0.5 g/L DCF with 3500 U/L laccases were analyzed using differential scanning calorimetry (DSC). The DSC instrument used was a Mettler-Toledo DSC-1. Under nitrogen atmosphere, the 6.4 mg sample was rapidly heated from 50 °C to 200 °C, kept at 200 °C for 15 minutes and then cooled at −10 °C/min from 200 °C to 50 °C. The glass transition temperature (T_g) was determined as the temperature of the inflexion point of the glass transition curve obtained during the cooling step [28, 29]. Laccases and DCF alone were analyzed following the same procedure for comparison purpose.

3. Calculation

3.1. Reaction scheme and assumptions

The developed model is based on a classical free-radical polymerization [30] with some modifications. In a classical free-radical polymerization, the first step, called the initiation, consists in the addition of an initiator that decomposes to form free radicals. These radicals then react with the monomer to form a free radical that will further react and polymerize [30].

In the present case, the initiation step is the reaction between the DCF monomer (DCF) and the laccase (E). It directly leads to the formation of the free radical (R_1) (reaction {1}). The next steps are the propagation of the polymerization (reaction {2}) leading to radical R_i composed of i DCF and the terminaison (reaction {3}) that leads to a non reactive polymer (P_{jk}).

$$\mathrm{DCF} \xrightarrow{k_0\ E} R_1 \qquad \{1\}$$

$$R_i + \mathrm{DCF} \xrightarrow{k_p} R_{i+1} \qquad \{2\}$$

$$R_j + R_k \xrightarrow{k_p} P_{jk} \qquad \{3\}$$

The following assumptions are used in this model:

- the initiation reaction follows a first order kinetic catalysed by the enzyme; saturation of the reaction rate as expected for Michaelian enzymes, is neglected,

- the rate constants of propagation and terminaison are independent of the size of the radicals and are the same for propagation and terminaison, these two steps are not catalysed by the laccase,
- the terminaison step leads to the precipitation of the polymer,
- other mechanisms classically considered in radical polymerization (transfer of the radical to the solvent, transfer to a monomer or transfer to another species) are neglected,
- insoluble byproducts are considered to be the only final products of the reaction.

3.2. Balance equation and resolution

Based on the assumptions presented in the previous section, the balance equations write:

$$\frac{dDCF}{dt} = -k_0\, E\, DCF - k_p\, DCF \sum_{l=1}^{\infty} R_l \tag{1}$$

$$\frac{dR_1}{dt} = k_0\, E\, DCF - k_p\, DCF\, R_1 - k_p\, R_1 \sum_{l=1}^{\infty} R_l \tag{2}$$

$$\frac{dR_i}{dt} = k_p\, DCF\, (R_{i-1} - R_i) - k_p\, R_i \sum_{l=1}^{\infty} R_l \text{ for } i = 2, ..., \infty \tag{3}$$

$$P = DCF_0 - \sum_{l=1}^{\infty} R_l - DCF \tag{4}$$

where t is the time (s), DCF is the mass concentration of DCF ($\mathrm{g\,L^{-1}}$), R_i is the mass concentration of the radical composed of i unit of DCF ($\mathrm{g\,L^{-1}}$), P is the total mass concentration of insoluble polymers ($\mathrm{g\,L^{-1}}$), k_0 is the kinetic constant of the enzymatic reaction of initiation ($\mathrm{L\ U^{-1}\ s^{-1}}$), E is the enzyme activity concentration ($\mathrm{U\ L^{-1}}$), k_p is the kinetic constants of propagation and terminaison ($\mathrm{L\,g^{-1}\,s^{-1}}$) and DCF_0 is the initial mass concentration of DCF ($\mathrm{g\,L^{-1}}$).

This set of equations can be reformulated by summing equations (2) and (3) for all the values of i, assuming that $R_\infty = 0$ and defining the total amount of radicals R^*:

$$R^* = \sum_{i=1}^{\infty} R_i \tag{5}$$

The system of equations then becomes:

$$\frac{dDCF}{dt} = -k_0\, E\, DCF - k_p\, DCF\, R^* \tag{6}$$

$$\frac{dR^*}{dt} = k_0\, E\, DCF - k_p\, R^{*2} \tag{7}$$

$$P = DCF_0 - R^* - DCF \tag{8}$$

The corresponding initial conditions at $t = 0$ are $DCF = DCF_0$, $R^* = 0$ and $P = 0$. This set of equations can be solved analytically by further assuming that the total amount of radicals is in pseudo-steady state:

$$\frac{dR^*}{dt} = 0 \tag{9}$$

The solution then writes:

$$R^* = \sqrt{\frac{k_0\,E}{k_p} DCF} \tag{10}$$

$$-k_0\,E\,t = \ln\left(\frac{DCF}{DCF_0}\right) - 2\,\ln\left(\frac{\sqrt{\frac{k_0\,E}{k_p DCF_0}} + \sqrt{\frac{DCF}{DCF_0}}}{\sqrt{\frac{k_0\,E}{k_p\,DCF_0}} + 1}\right) \tag{11}$$

$$\frac{P}{DCF_0} = 1 - \frac{DCF}{DCF_0} - \sqrt{\frac{k_0\,E}{k_p\,DCF_0}}\sqrt{\frac{DCF}{DCF_0}} \tag{12}$$

Under this form, the model has 2 adjustable kinetic constants (k_0 and k_p) as only parameters of unknown value.

3.3. Non-dimensional form

The set of equations (10),(11) and (12) can be rewritten in non-dimensional form by introducing the DCF conversion X, the non-dimensional time of reaction τ and a non-dimensional parameter θ :

$$\theta = \sqrt{\frac{k_0\,E}{k_p DCF_0}} \tag{13}$$

$$\tau = k_0\,E\,t \tag{14}$$

$$X = 1 - \frac{DCF}{DCF_0} \tag{15}$$

The θ constant is a non-dimensional number that compares the order of magnitude of initiation reaction rate and terminaison reaction rate. A large value of θ means that the appearance of IBs is delayed compared to the consumption of DCF. The other way around, a small value of θ indicates a formation of IBs that is limited by the enzymatic initiation.

With these definitions, the set of equations (10), (11) and (12) can be written :

$$\frac{R^*}{DCF_0} = \theta\sqrt{1 - X} \tag{16}$$

$$\tau = 2\,\ln\left(\frac{\theta + \sqrt{1 - X}}{\theta + 1}\right) - \ln(1 - X) \tag{17}$$

$$\frac{P}{DCF_0} = X - \theta\sqrt{1 - X} \tag{18}$$

3.4. Parameters adjustment

The kinetic constants were adjusted step by step. First, the invariant part of θ ($\sqrt{k_0/k_p}$) was adjusted by fitting the $\frac{P}{DCF_0}$ values predicted by eq. (18) on experimental values using the least squares method. Values for X ranging from 0.2 to 0.7 and the corresponding values of $\frac{P}{DCF_0}$ from experiments EXP1 and EXP2 were used for this adjustment.

Then, k_0 value was adjusted by fitting the t values predicted by eq. (17) using the determined θ values and experimental values of X and comparing those t values to the experimental ones using the least squares method. The data from experiments EXP1 and EXP2 were used for this adjustment. The values corresponding to 24h of experiment were excluded from the adjustment.

Finally, the value of k_p was calculated using eq. (13).

3.5. Analysis of features of the kinetic model

Some features of the model can be highlighted by manipulating the different sets of equations in order to simplify the analysis and discuss important design rules.

3.5.1. Minimum conversion for IBs formation

Eq. (18) shows that the relationship between the conversion and the fraction of DCF that was insolubilized only depends on θ. This equation can also by manipulated to highlight a minimum conversion X_{min} for IBs formation. Indeed, for $0 < X < X_{min}$, eq. (18) gives a negative value of $\frac{P}{DCF_0}$, which has no physical meaning. As long as $X < X_{min}$, the assumption of quasi-steady state of the total radical concentration is not valid as too few DCF as reacted to reach the quasi steady state quantity of radicals. From eq. (18), X_{min} value can be isolated as :

$$X_{min} = -\frac{\theta^2}{2} + \theta\frac{\sqrt{\theta^2+4}}{2} \tag{19}$$

For the time corresponding to $0 < X < X_{min}$, no IBs should be observed, P is forced to zero in the model. This phase is further referred to as a lag phase.

3.5.2. Impact of the polymerization on the reaction time

The consumption of DCF by radicals accelerates the reaction rate compared to a situation where only the enzymatic reaction degrades DCF. To quantity this impact, the reaction time τ_0 needed to reach the conversion X if DCF was only reacting following reaction {1} can be calculated:

$$\tau_0 = -\ln(1-X) \tag{20}$$

Combining (20) and (17) allows to isolate acceleration factor due to the polymerization reaction as:

$$A = \frac{\tau_0}{\tau} = \left[1 - \frac{2\,\ln\left(\frac{\theta+\sqrt{1-X}}{\theta+1}\right)}{\ln(1-X)}\right]^{-1} \tag{21}$$

3.5.3. Further reaction after inactivation of the enzyme

The free-radical polymerization scheme has for consequence that even if no new radical is produced, the polymerization continues until no further reactant is available. Therefore in the present case, if enzyme activity stops, DCF conversion keeps on. Enzymatic activity might be suppressed by enzyme inactivation or, in continuous reactor, because the reaction mix leaves the region where enzyme is present.

Assuming that at $t = t_s$ the enzymatic activity is instantaneously switched from its initial value to zero, the corresponding conversion X_s, amount of radicals R_s^* and IBs quantity P_s can be calculated at time t_s using equations (16),(17) and (18).

The evolution of conversion of DCF and IBs production over time after t_s can be evaluated by manipulating the set of equations (6) and (7) with $E = 0$ and without assuming a steady-state quantity of radical. The analytical solution writes in non-dimensional form:

$$\frac{R^*}{DCF_0} = \frac{\theta^2\sqrt{1-X_s}}{\theta + \sqrt{1-X_s}\,(\tau - \tau_s)} \tag{22}$$

$$X = 1 - \frac{\theta\,(1-X_s)}{\theta + \sqrt{1-X_s}\,(\tau - \tau_s)} \tag{23}$$

where $\tau_s = k_0 E t_s$.

4. Results and Discussion

4.1. Determination of the kinetic constants

The values determined for the kinetic constants are presented in Table 2. The corresponding values of θ for the different experimental conditions are summarized in Table 1.

The highest θ value obtained was that of EXP7. From a mechanism perspective, a high θ value corresponds to an appearance of IBs delayed compared to DCF consumption. Indeed, in EXP7, as DCF was consumed, no IBs formation was observed during the 6h of reaction.

DISCUTER VALEURS THETA? PLUS? MOINS?

Table 2: Adjusted values of the kinetic constants used in the model.

k_0 (L U^{-1} s^{-1})	k_p (L g^{-1} s^{-1})
$2.26\,10^{-9}$	$2.08\,10^{-4}$

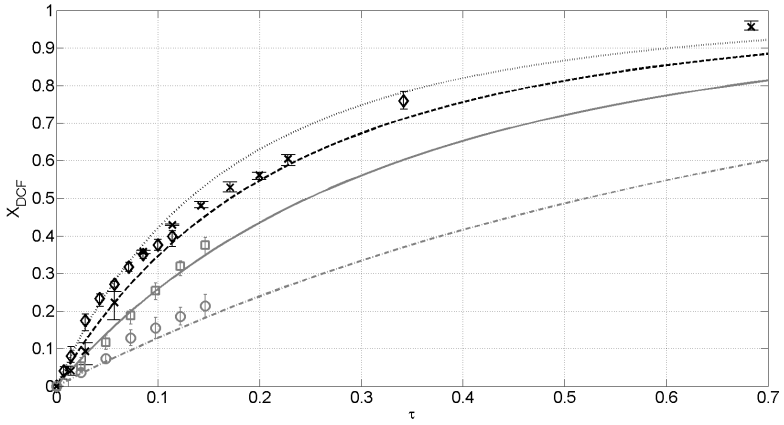

Figure 1: Evolution of DCF removal over time multiplied by enzymatic activity. Several sets of experimental conditions are displayed: 0.5 g DCF/L + 3500 U/L: '×' = experimental data, '- -' = model; 0.5 g DCF/L + 1750 U/L: '◊' = experimental data, '...' = model. Error bars display the differences between the maximum/minimum values and the average values.

4.2. Experimental Degradation of DCF and IBs Formation

4.2.1. DCF degradation by Laccases

DCF is removed by the laccase and its removal is dependent of time, enzymatic activity and the initial concentration of DCF (DCF_0) present in solution. Using an initial concentration of 0.5 g DCF/L, we attain removals of 35% and 76% after 6h and 24h of reaction with 1750 U/L (EXP2) and removals of 53% and 96% after 6h and 24h of reaction with 3500 U/L (EXP1). After 6h of reaction with 3000 U/L, DCF removal is found to be 21% for a DCF_0 of 0.005 g/L (EXP7) and 38% for a DCF_0 of 0.15 g/L (EXP6).

The dependence of the removal on laccase activity is directly related to reaction {1}. More laccases present in solution means more laccase-catalyzed oxidation of DCF to form radicals. The dependence of the removal on DCF_0 can be explained through LIEN AVEC THETA ET POLYMERISATION?

The model presented in section 3 allows for a good prediction of the removal of DCF. Even for conditions sets presenting DCF concentrations much lower than those used for the adjustment of parameters.

4.2.2. Relations between DCF degradation and IBs Formation

The comparison between experimental values of DCF removal and the proportion of DCF turned into IBs shows the presence of the 'lag phase' described in Section 3 (see Figure 2). It appears that only a really small amount of DCF is turned into IBs until a DCF degradation of 20-25% is reached, which is coherent with the X_{min} values presented in Table 1. Then, the amount of DCF turned into IBs increases rapidly to reach a conversion into IB of 78% for 96% of DCF removal.

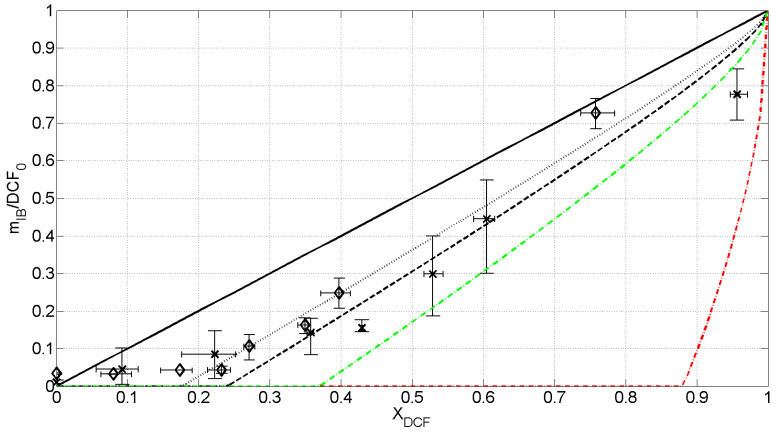

Figure 2: Evolution of IBs formation in function of DCF degradation. Error bars display the differences between the maximum/minimum values and the average values. Several sets of conditions are displayed: '–' = theoretical case with DCF instantly transformed in IB; 0.5 g DCF/L + 3500 U/L: '×' = experimental data (average value of 3 experiments for DCF and average values of 5 experiments for IB), '- -' = model; 0.5 g DCF/L + 1750 U/L: '◊' = experimental data (average values of 3 experiments for DCF and average values of 3 experiments for IB), '...' = model.

As explained in Section 3, the 'lag phase' corresponds to a range of DCF removal for which the assumption of a quasi steady state of radicals concentration is not valid. In that range of DCF removal ($X < X_{min}$), the amount of DCF transformed into radical is not sufficient to meet the assumption of a quasi steady state of radicals concentration. From a mechanism point of view, that would correspond to the fact that, at these values of DCF conversion, the concentrations of DCF and radicals make the propagation of the polymerization reaction (see reaction {2}) more likely to occur than its terminaison (see reaction {3}) leading to an increase in DCF degradation without any important IBs formation.

DISCUTER L'AUGMENTATION RAPIDE DE IB QUI SUIT LA LAG PHASE?

4.2.3. Kinetics of IBs Formation

During DCF degradation, it was observed that the color of the medium shifted from colorless to yellow, then orange and finally brown along with the formation of insoluble byproducts that precipitated. That kind of behavior was described in literature while dealing with DCF oxidation (see Table 3). That color change and IBs formation was observed for all conditions sets with the exception of EXP7.

Concerning the kinetics of formation of these brown-colored precipitates, 2 phases are observed (see Figure 3). METTRE LES PHASES SUR LA FIGURE.

First, the lag phase detailed in Sections 3 and 4.2.2 is observed for τ values

Table 3: Color change and formation of precipitates reported in literature during degradation of DCF.

Degradation method used	Observed phenomena	Identified transformation products	Ref.
T. versicolor laccase	Transformation product of yellow color, precipitate formation		[23]
T. versicolor laccase	Mixture color shifted from colorless to brown	4-(2,6-dichlorophenylamino)-1,3-benzenedimethanol	[19]
Thielavia laccase	Formation of polymerization products	dimers, trimers, tetramers, pentamers and hexamers	[24]
Horseradish peroxidase	Formation of a product of dark orange color		[31]
Horseradish peroxidase	Reaction mixture turned yellow	dimers	[32]
Myeloperoxidase	Formation of an orange precipitate	dihydroxyazobenzene	[33]
UV photolysis	Formation of brown-colored dimers	dimers	[34]

ranging from 0 to 0.06. Then, a phase of fast rise of the proportion of DCF transformed into IBs is observed.

The proportion of DCF transformed into IBs increased with the enzymatic activity. Using a DCF_0 of 0.5 g/L, the proportion of DCF transformed into IBs after 24h of reaction was 42% with 1200 U/L (EXP3), 73% with 1750 U/L (EXP2) and 78% with 3500 U/L (EXP1). The experimental relation between the proportion of DCF transformed into IBs and the initial concentration of DCF in solution was less clear. Using an enzymatic activity of 1750 U/L, the proportion of DCF transformed into IBs after 24h of reaction was 53% with a DCF_0 of 0.25 g/L, 44% with a DCF_0 of 0.375 g/L and 73% with a DCF_0 of 0.5 g/L (see Fig. 3).

Experimentally, the lag phase shows a small quantity of IBs while the model predicts a total absence of IBs. That difference between model and experimental data is caused by the fact that, at this point, the assumption of a quasi steady state of radicals concentration is not valid. Indeed, at the start of the reaction, the total amount of radicals is growing but not yet as important as when it becomes constant.

The model gives a good prediction of the formation of IBs for EXP1 and EXP2. The results of the model for EXP5 are less convincing and the formation of IBs during EXP3 and EXP4 is overestimated. That difference can be linked to the fact that the masses of IBs experimentally recovered for EXP3, EXP4 and EXP5 were smaller than those recovered during EXP1 and EXP2 and then more prone to non-significant measurements (mass value inferior to the controls)

Table 4: Temperature of the glass transition of IBs obtained through the reaction of 0.5 g DCF/L and 3500 U/L.

Reaction time (h)	T_g (°C)
6	135
8	140
24	138

and to imprecision in measurement.

The t_{min} values predicted using eq. (19) and (17) obtained for EXP1 and EXP2 are in concordance with the experimental results (see t_{min} values in Table 1 and Fig. 3). Values of t_{min} obtained for the other tests appear quite smaller than what is observed experimentally. The explanation is the same than for the difference between measured and modeled amounts of IBs: as EXP3, EXP4 and EXP5 were performed using smaller amounts of DCF, they were more sensitive to noise during measurement.

LAISSER PARAGRAPHE SUR tmin? SI OUI, FAIRE DONNER LES VALEURS DE THETA CORRESPONDANTES (AU MOINS DANS PARAGRAPHE), SI NON, RETIRER DU TABLEAU

4.2.4. IBs Characterization

The DSC analysis performed on some of the formed IBs showed the presence of a slight glass transition between 120 °C and 160 °C (see Figure 4). As no glass transition is observable in the DCF and laccase alone analyzes, this transition is characteristic of the IBs. Polymers can be characterized using their temperature of glass transition. So, the fact that the formed IBs present a glass transition suggest that they are of polymeric nature which agrees with literature (see Table 3).

There seems to be no real evolution of T_g through time (see Table 4). That suggests that the IBs composition is such that their average T_g is constant.

4.3. Features of the Model

4.3.1. Minimum Conversion for IBs Formation

The minimum conversion for IBs formation, X_{min}, presented in eq. (19), represents the DCF conversion that has to be reached for the assumption of quasi-steady state of the total radical concentration to be valid. The value of X_{min} is only depending on the value of θ (see Fig. 5). X_{min} increases with the increase of the value of θ. For $\theta < 0.01$, X_{min} is close to zero, expressing the direct precipitation of polymers when DCF is consumed. For $\theta > 10$, X_{min} is close to one, delaying the apparition of IBs.

4.3.2. Acceleration Factor

The acceleration factor (A) represents how much the consumption of DCF by radicals accelerates the reaction rate compared to a situation where only

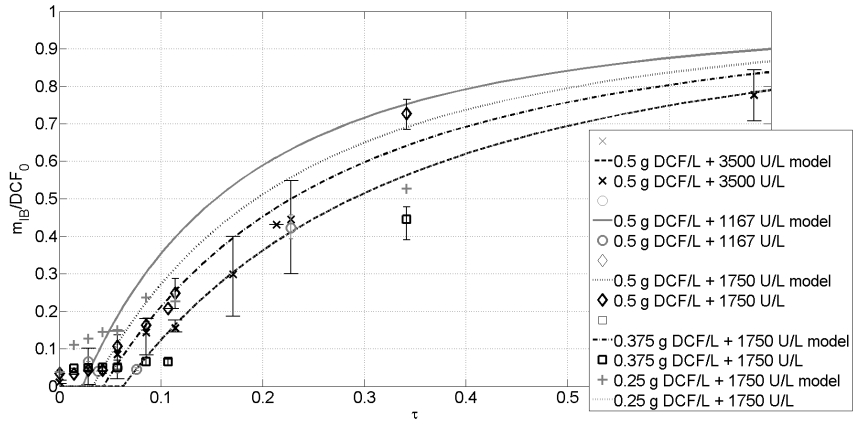

(a) 24 hours reaction.

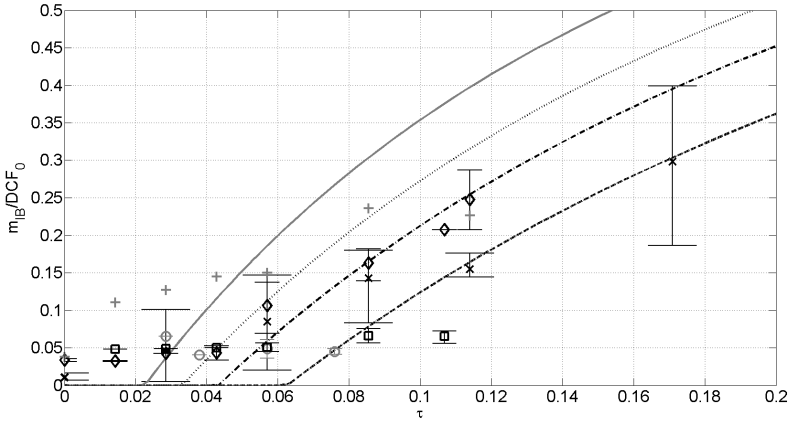

(b) Focus on the early stage of the reaction.

Figure 3: Evolution of IBs formation over time multiplied by enzymatic activity. Several sets of experimental conditions are displayed. Experimental data are average values of 5, 3, 3 and 3 experiments for 0.5 g DCF/L + 3500 U/L, 0.5 g DCF/L + 1167 U/L, 0.5 g DCF/L + 1750 U/L and 0.375 g DCF/L + 1750 U/L respectively. Error bars display the differences between the maximum/minimum values and the average values.

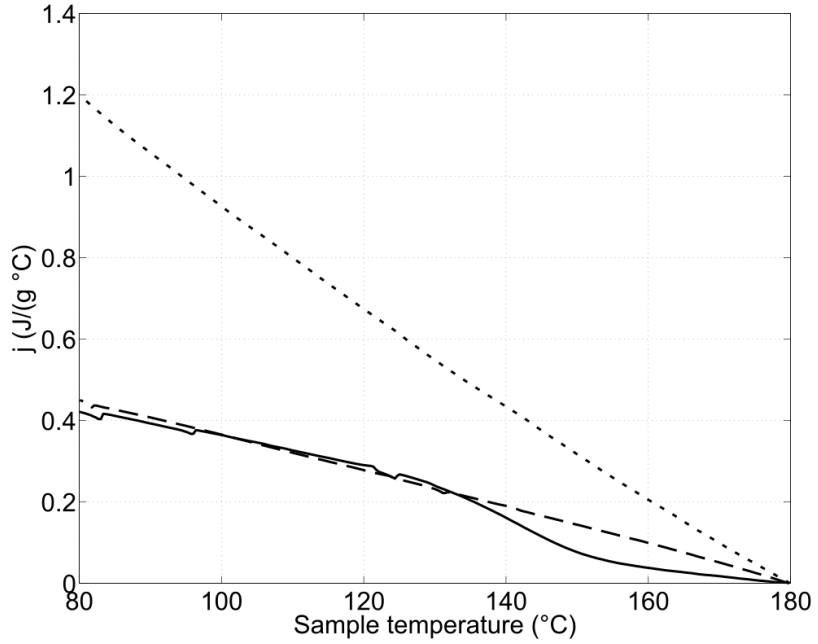

Figure 4: Results of DSC analyzes. For readability purposes, the curves were translated so they all equal $0\,\mathrm{J\,g^{-1}\,°C^{-1}}$ at 180 °C. Full line = IBs (glass transition visible between 120 °C and 160 °C); Dashes = DCF; Doted line = laccases.

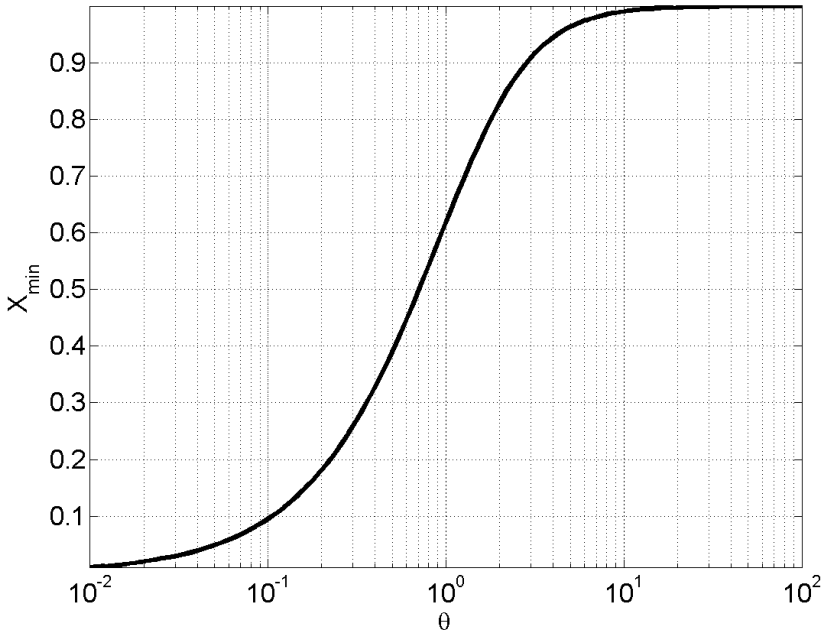

Figure 5: Evolution of the minimum conversion to observe IBs as a function of θ.

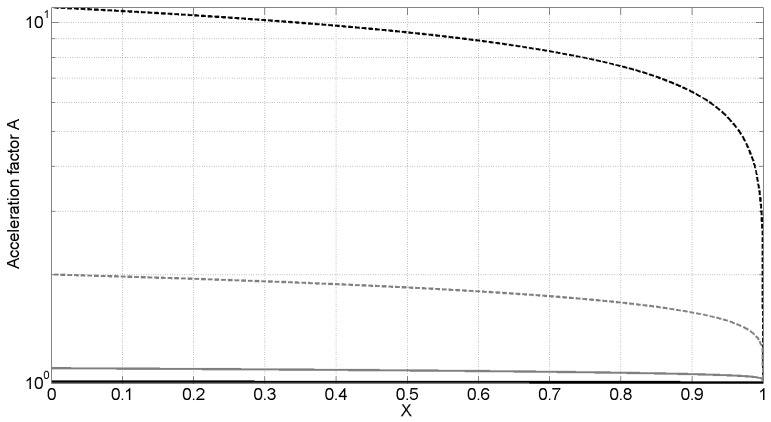

Figure 6: Evolution of the acceleration factor due to the polymerization reaction (A) in function of the conversion of DCF (X) for several value of θ. The dotted black line represents the evolution of A for $\theta = 0.1$. The dotted gray line represents the evolution of A for $\theta = 1$. The plain gray line represents the evolution of A for $\theta = 10$. The plain black line represents the evolution of A for $\theta = 100$.

the enzymatic reaction degrades DCF. It is at the start of the reaction, when X values are small, that the value of A is the highest. However, the A value can remain quite high for most of the reaction (see Fig. 6). At the end of the reaction, when X value tends to 1, the A value decreases strongly to reach 1 as well. This represents the fact that, at this point, too few DCF remains in solution for the polymerization to occur.

The A value is shown to strongly depends on the θ value, as the consumption of DCF by radicals accelerates more than ten times the reaction rate for a θ value of 0.1 but a θ value of 100 corresponds to no real acceleration (A=1.01) (see Fig. 6).

4.3.3. Further Reaction After Inactivation of the Enzyme

After the inactivation of the enzyme that stops the reaction {1}), the reactions of propagation (reaction {2}) and terminaison (reaction {3}) of the polymerization can still occur while there are enough radicals in solution. Through reaction {2}, the conversion of DCF can keep going, even if the enzyme is not active anymore.

The conversion that can be reached after the inactivation of the enzyme depends of θ and X_s, the value of conversion already reached when the enzyme is inactivated. Indeed, the rate of this reaction decreases when θ and X_s values increase (see Fig. 7).

This effect can be responsible for some noise on the conversions that we measured experimentally. However, given the θ values with which we worked and the short time between the inactivation of the enzyme and the HPLC analyses, that noise can generate an error of no more than 1% on the measured

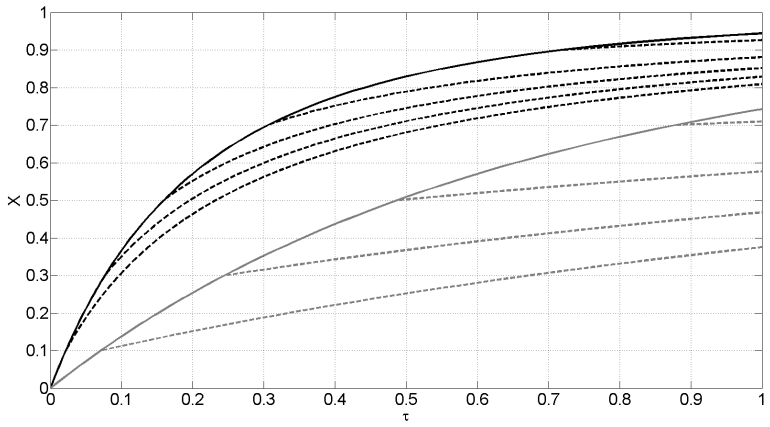

Figure 7: Evolution of the conversion of DCF (X) after the inactivation of the enzyme through polymerization by already formed radicals (according to eq. (23)). The lines correspond $\theta = 0.25$. The gray lines correspond to $\theta = 2$. The plain lines correspond to conversion while the enzyme is active. The dotted lines correspond to conversion past inactivation (for different values of conversion at the time of inactivation, X_s).

conversions.

4.4. Information for Design and Scale-up

Two elements have to be taken into account regarding the reaction time needed to attain a given conversion and the possibility of IBs formation: $k_0\,E$ and θ.

To reduce the reaction time needed to reach a given conversion, the key is to augment the value of $k_0\,E$. The value of k_0 depends on the enzyme, so for a given enzyme that translates to increase E. Increasing E will make the reaction faster but also increase the θ value which will, in turn, increase X_{min} value. These increases in θ and X_{min} values mean that the formation of IBs will be improbable, meaning that there will be no substantial gain of removal through polymerization but that no formation of IBs will impair the process (by clogging the reactor for instance).

Another case to consider is that of a limited supply of enzyme. In this case, the E value will probably be quite smaller, resulting in a small value of θ and the possibility for the polymerization reaction to play a more important role in DCF removal (see the acceleration factors in Fig. 6).

In real conditions, the highest concentration of DCF measured in WWTP effluents is $5.5\,\mu g\,L^{-1}$ [3]. Considering an hypothetical use of 3000 U/L of the same laccase that the one studied here (*T. versicolor*), such a value of DCF_0 would give a θ value of 77, meaning that the impact of the polymerization on DCF removal would be negligible (see Fig. 6). Moreover, a real WWTP effluent represents a mix of various compounds, not just DCF, so DCF radicals would be likely to react with compounds other than DCF.

5. Conclusion

The degradation of DCF by laccases leads to the formation of brown-colored IBs. These IBs are probably formed through a form of free-radical polymerization, whit the enzymatically-formed free radicals of DCF reacting whit each other. According to results found in literature, these IBs are probably small oligomers [24, 32]. However, they are not the only products formed through the reaction. Soluble products are probably also formed as there is no complete transformation of DCF into IBs. Also, the IBs formation seems to need a minimum conversion of DCF to occur.

AJOUTER UNE PARTIE SUR LE MODELE

Acknowledgments

Rosalie Pype acknowledges financial support from the Fonds de la Recherche Scientifique - FNRS in the form of a grant of the Fonds pour la Formation à la Recherche dans l'Industrie et dans l'Agriculture (FRIA), Brussels, Belgium.

Conflicts of interest

The authors declare that they have no conflicts of interest.

[1] V. Acuña, A. Ginebreda, J. R. Mor, M. Petrovic, S. Sabater, J. P. Sumpter, and D. Barceló. Balancing the health benefits and environmental risks of pharmaceuticals: Diclofenac as an example. *Environ. Int.*, 85:327–333, December 2015. doi: 10.1016/j.envint.2015.09.023.

[2] P. McGettigan and D. Henry. Use of Non-Steroidal Anti-Inflammatory Drugs That Elevate Cardiovascular Risk: An Examination of Sales and Essential Medicines Lists in Low-, Middle-, and High-Income Countries. *PLoS Med.*, 10(2):e1001388, February 2013. doi: 10.1371/journal.pmed.1001388.

[3] N. Vieno and M. Sillanpää. Fate of diclofenac in municipal wastewater treatment plant — A review. *Environ. Int.*, 69:28–39, August 2014. doi: 10.1016/j.envint.2014.03.021.

[4] Y. Zhang, S.-U. Geißen, and C. Gal. Carbamazepine and diclofenac: Removal in wastewater treatment plants and occurrence in water bodies. *Chemosphere*, 73(8):1151–1161, November 2008. doi: 10.1016/j.chemosphere.2008.07.086.

[5] R. A. Triebskorn, H. Casper, A. Heyd, R. Eikemper, H.-R. Köhler, and J. Schwaiger. Toxic effects of the non-steroidal anti-inflammatory drug diclofenac: Part II. Cytological effects in liver, kidney, gills and intestine of rainbow trout (*Oncorhynchus mykiss). Aquat. Toxicol.*, 68(2):151–166, June 2004. doi: 10.1016/j.aquatox.2004.03.015.

[6] J. Schwaiger, H. Ferling, U. Mallow, H. Wintermayr, and R. D. Negele. Toxic effects of the non-steroidal anti-inflammatory drug diclofenac: Part I: hystopathological alterations and bioaccumulation in rainbow trout. *Aquat. Toxicol.*, 68(2):141–150, June 2004. doi: 10.1016/j.aquatox.2004.03.014.

[7] M. Lahti, J.-M. Brozinski, A. Jylhä, L. Kronberg, and A. Oikari. Uptake from water, biotransformation, and biliary excretion of pharmaceuticals by rainbow trout. *Environ. Toxicol. Chem.*, 30(6):1403–1411, June 2011. doi: 10.1002/etc.501.

[8] B. Huerta, A. Jakimska, M. Llorca, A. Ruhí, G. Margoutidis, V. Acuña, S. Sabater, S. Rodriguez-Mozaz, and D. Barcelò. Development of an extraction and purification method for the determination of multi-class pharmaceuticals and endocrine disruptors in freshwater invertebrates. *Talanta*, 132:373–381, January 2015. doi: 10.1016/j.talanta.2014.09.017.

[9] T. Backhaus, J. Sumpter, and H. Blanck. On the Ecotoxicology of Pharmaceutical Mixtures. In *Pharmaceuticals in the Environment*, pages 257–276. Springer, Berlin, Heidelberg, 2008.

[10] M. I. Vasquez, A. Lambrianides, M. Schneider, K. Kümmerer, and D. Fatta-Kassinos. Environmental side effects of pharmaceutical cocktails: What we know and what we should know. *J. Hazard. Mater.*, 279:169–189, August 2014. doi: 10.1016/j.jhazmat.2014.06.069.

[11] M. Cleuvers. Mixture toxicity of the anti-inflammatory drugs diclofenac, ibuprofen, naproxen, and acetylsalicylic acid. *Ecotox. Environ. Safe.*, 59 (3):309–315, November 2004. doi: 10.1016/S0147-6513(03)00141-6.

[12] U. N. Dwivedi, P. Singh, V. P. Pandey, and A. Kumar. Structure–function relationship among bacterial, fungal and plant laccases. *J. Mol. Catal. B Enzym.*, 68(2):117–128, February 2011. doi: 10.1016/j.molcatb.2010.11.002.

[13] P. Giardina, V. Faraco, C. Pezzella, A. Piscitelli, S. Vanhulle, and G. Sannia. Laccases: a never-ending story. *Cell. Mol. Life Sci.*, 67(3):369–385, February 2010. doi: 10.1007/s00018-009-0169-1.

[14] J.-A. Majeau, S. K. Brar, and R. D. Tyagi. Laccases for removal of recalcitrant and emerging pollutants. *Bioresour. Technol.*, 101(7):2331–2350, April 2010. doi: 10.1016/j.biortech.2009.10.087.

[15] H. Claus. Laccases: structure, reactions, distribution. *Micron*, 35(1-2): 93–96, January 2004. doi: 10.1016/j.micron.2003.10.029.

[16] C. Hautphenne, M. Penninckx, and F. Debaste. Product formation from phenolic compounds removal by laccases: A review. *Environ. Technol. Innov.*, 5:250–266, April 2016. doi: 10.1016/j.eti.2016.04.001.

[17] R. R. Nair, P. Demarche, and S. N. Agathos. Formulation and characterization of an immobilized laccase biocatalyst and its application to eliminate organic micropollutants in wastewater. *New Biotechnol.*, 30(6):814–823, September 2013. doi: 10.1016/j.nbt.2012.12.004.

[18] L. Lloret, G. Eibes, T. A. Lú-Chau, M. T. Moreira, G. Feijoo, and J. M. Lema. Laccase-catalyzed degradation of anti-inflammatories and estrogens. *Biochem. Eng. J.*, 51(3):124–131, September 2010.

[19] E. Marco-Urrea, M. Pérez-Trujillo, C. Cruz-Morató, G. Caminal, and T. Vicent. Degradation of the drug sodium diclofenac by *Trametes versicolor* pellets and identification of some intermediates by NMR. *J. Hazard. Mater.*, 176(1-3):836–842, April 2010. doi: 10.1016/j.jhazmat.2009.11.112.

[20] L. Lloret, G. Eibes, M. T. Moreira, G. Feijoo, and J. M. Lema. On the use of a high-redox potential laccase as an alternative for the transformation of non-steroidal anti-inflammatory drugs (NSAIDs). *J. Mol. Catal. B Enzym.*, 97:233–242, December 2013. doi: 10.1016/j.molcatb.2013.08.021.

[21] L. N. Nguyen, F. I. Hai, W. E. Price, F. D. L. Leusch, F. Roddick, E. J. McAdam, S. F. Magram, and L. D. Nghiem. Continuous biotransformation of bisphenol A and diclofenac by laccase in an enzymatic membrane reactor. *Int. Biodeterior. Biodegradation*, 95:25–32, November 2014. doi: 10.1016/j.ibiod.2014.05.017.

[22] R. Xu, R. Tang, Q. Zhou, F. Li, and B. Zhang. Enhancement of catalytic activity of immobilized laccase for diclofenac biodegradation by carbon nanotubes. *Chem. Eng. J.*, 262:88–95, February 2015. doi: 10.1016/j.cej.2014.09.072.

[23] J. Margot, J. Maillard, L. Rossi, D. A. Barry, and C. Holliger. Influence of treatment conditions on the oxidation of micropollutants by *Trametes versicolor* laccase. *New Biotechnol.*, 30(6):803–813, September 2013. doi: 10.1016/j.nbt.2013.06.004.

[24] G. Hommes, C. A. Gasser, E. M. Ammann, and P. F.-X. Corvini. Determination of Oxidoreductase Activity Using a High-Throughput Microplate Respiratory Measurement. *Ana. Chem.*, 85(1):283–291, January 2013. doi: 10.1021/ac302716j.

[25] G. Gomori. Preparation of buffers for use in enzyme studies. In *Methods in Enzymology*, volume 1, pages 138–146. Elsevier, 1955.

[26] H. U. Bergmeyer and K. Gawehn, editors. *Principles of Enzymatic Analysis*. Verlag Chemie, New York, 1978.

[27] C. Hautphenne and F. Debaste. Harnessing Laccases for the Synthesis of Bisphenol A Biopolymers. *Chem. Eng. Technol.*, 38(7):1223–1228, July 2015. doi: 10.1002/ceat.201400629.

[28] P. Claudy. *Analyse calorimétrique différentielle: Théorie et applications de la d.s.c.* Editions TEC & DOC : Lavoisier, Paris; Londres, 2005.

[29] G. Höhne, W. Hemminger, and H.-J. Flammersheim. *Differential scanning calorimetry: an introduction for practitioners*. Springer, Berlin ; New York, 2nd rev. and enl. ed edition, 2003.

[30] Hugh Scott Fogler. *Elements of chemical reaction engineering*. Prentice Hall International, Upper Saddle River, New Jersey, 3. ed., internat. ed edition, 1999.

[31] C. Huber, M. Preis, P. J. Harvey, S. Grosse, T. Letzel, and P. Schröder. Emerging pollutants and plants – Metabolic activation of diclofenac by peroxidases. *Chemosphere*, 146:435–441, March 2016. doi: 10.1016/j.chemosphere.2015.12.059.

[32] L. F. Stadlmair, T. Letzel, J. E. Drewes, and J. Graßmann. Mass spectrometry based in vitro assay investigations on the transformation of pharmaceutical compounds by oxidative enzymes. *Chemosphere*, 174:466–477, May 2017. doi: 10.1016/j.chemosphere.2017.01.140.

[33] K. W. M. Zuurbier, A. R. J. Bakkenist, R. H. Fokkens, N. M. M. Nibbering, R. Wever, and A. O. Muijsers. Interaction of myeloperoxidase with diclofenac. *Biochem. Pharmacol.*, 40(8):1801–1808, October 1990. doi: 10.1016/0006-2952(90)90359-S.

[34] O. S. Keen, E. M. Thurman, I. Ferrer, A. D. Dotson, and K. G. Linden. Dimer formation during UV photolysis of diclofenac. *Chemosphere*, 93(9): 1948–1956, November 2013. doi: 10.1016/j.chemosphere.2013.06.079.